Title

Delineation of biomarkers and molecular pathways of residual effects of fluoxetine treatment in juvenile rhesus monkeys by proteomic profiling

Journal

动物学研究, 44(1)

ISSN

2095-8137

Authors

Yan, Yu

Park, Dong Ik

Horn, Anja

et al.

Publication Date

2023

DOI

10.24272/j.issn.2095-8137.2022.196

Yan et al. *Zool. Res.* 2023, 44(1): 30−42
https://doi.org/10.24272/j.issn.2095-8137.2022.196

ZR | Zoological Research

Article Open Access

Delineation of biomarkers and molecular pathways of residual effects of fluoxetine treatment in juvenile rhesus monkeys by proteomic profiling

Yu Yan[1], Dong Ik Park[1,†], Anja Horn[2], Mari Golub[3], Christoph W. Turck[1,*]

[1] *Proteomics and Biomarkers*, *Max Planck Institute of Psychiatry*, *Munich* 80804, *Germany*
[2] *Ludwig-Maximilians-Universität*, *Chair of Vegetative Anatomy*, *Institute of Anatomy*, *Faculty of Medicine*, *Munich* 80336, *Germany*
[3] *Department of Environmental Toxicology*, *University of California*, *Davis*, *CA* 95616, *USA*

ABSTRACT

Fluoxetine (Prozac™) is the only antidepressant approved by the US Food and Drug Administration (FDA) for the treatment of major depressive disorder (MDD) in children. Despite its considerable efficacy as a selective serotonin reuptake inhibitor, the possible long-term effects of fluoxetine on brain development in children are poorly understood. In the current study, we aimed to delineate molecular mechanisms and protein biomarkers in the brains of juvenile rhesus macaques (*Macaca mulatta*) one year after the discontinuation of fluoxetine treatment using proteomic and phosphoproteomic profiling. We identified several differences in protein expression and phosphorylation in the dorsolateral prefrontal cortex (DLPFC) and cingulate cortex (CC) that correlated with impulsivity in animals, suggesting that the GABAergic synapse pathway may be affected by fluoxetine treatment. Biomarkers in combination with the identified pathways contribute to a better understanding of the mechanisms underlying the chronic effects of fluoxetine after discontinuation in children.

Keywords: Major depressive disorder; Fluoxetine; Rhesus monkeys; Proteomics; GABAergic synapse

INTRODUCTION

Major depressive disorder (MDD) is a common mental illness affecting millions of people of all ages worldwide (Bromet et al., 2011). Although MDD also frequently occurs in children, fluoxetine, a selective serotonin reuptake inhibitor (SSRI), is the only currently available antidepressant approved by the US Food and Drug Administration (FDA) to treat pediatric depression in children (eight years and older) (Costello et al., 2003; Selph & Mcdonagh, 2019). Despite its significant pharmacological efficacy, there are no studies on the potential effects of fluoxetine on brain development in children. Notably, recent studies in nonhuman primates (NHPs) have documented persistent effects on sleep disturbance, sustained attention, and impulsivity after discontinuation of treatment (Golub et al., 2017; Golub & Hogrefe, 2016; Golub et al., 2016a; Golub et al., 2018; He et al., 2014). Furthermore, alterations in serotonin receptor binding and lipidomics have been detected in the brain one year after treatment cessation (Golub et al., 2019; Tkachev et al., 2021).

Mass spectrometry-based proteomics combined with

Received: 04 August 2022; Accepted: 18 October 2022; Online: 20 October 2022

Foundation items: This work was supported by the Max Planck Society to C.W.T. and National Institutes of Health USDHHS (R01-HD065826 to M.G., OD011107 to Harris Lewin)

[†]Current address: Aarhus University, Department of Biomedicine, 8000 Aarhus, Denmark

*Corresponding author, E-mail: turck@psych.mpg.de

bioinformatics analysis has great potential in disease diagnosis and prognosis, assessment of disease progression, drug and biomarker development, and mechanistic research. Several studies have investigated brain development in rodents using proteomic and phosphoproteomic approaches. Over 500 phosphorylation sites and potential phosphorylation binding motifs of critical proteins have been identified in the developing mouse brain (Ballif et al., 2004). Furthermore, over 1 300 proteins and 1 750 phosphorylation sites among three developmental states have been identified in other research, revealing developmentally dynamic proteomes and phosphoproteomes (Doubleday & Ballif, 2014). A multiregional quantitative proteomic survey of the postnatal human brain also discovered several clusters of temporally co-expressed proteins with increased or decreased expression during postnatal brain development (Carlyle et al., 2017).

NHPs are among the best models for translational research of MDD due to their high similarity with human brain structure, social behavior, and physiological development (Reite & Short, 1983). NHPs also contain many genetic polymorphisms that are associated with psychiatric disorders in humans. We previously found that chronic fluoxetine dosing can increase impulsivity in juvenile male rhesus macaques (*Macaca mulatta*), and further identified a set of potential metabolite biomarkers and changed metabolic pathways in the blood, cerebrospinal fluid (CSF), and peripheral fibroblasts of the animals (Golub et al., 2016b; He et al., 2014; Su et al., 2016).

In the present study, we examined the long-term effects of fluoxetine treatment on juvenile male rhesus monkeys using proteomic and phosphoproteomic profiling of the dorsolateral prefrontal cortex (DLPFC) and cingulate cortex (CC) brain regions, where the strongest post-fluoxetine treatment effects on brain serotonin transporter (SERT) are observed (Golub et al., 2019). In the proteomic study, we used monkeys with two common monoamine oxidase A (*MAOA*) gene polymorphisms previously associated with MDD (Schildkraut, 1965; Von Knorring et al., 1985). We identified several potential biomarkers suggesting involvement of the GABAergic synapse pathway in the increase in juvenile rhesus monkey impulsivity one year after discontinuation of fluoxetine therapy. Identifying protein biosignatures and affected pathways contributes to a better understanding of the impacts of chronic fluoxetine treatment on brain development in children.

MATERIALS AND METHODS

Animals, fluoxetine dosing, and behavioral testing

All procedures followed the Guide for the Care and Use of Laboratory Animals of the National Research Council. The California National Primate Research Center (CNPRC) is accredited by the Association for Assessment and Accreditation of Laboratory Animal Care. Protocols for this project were approved prior to implementation by the University of California (UC) Davis Institutional Animal Care and Use Committee (protocol #18008).

Male rhesus macaques were obtained from the breeding colony at one year of age, approximately equivalent to 4–6 years of age in human children. The subjects were identified as hemizygous for low-transcribing (seven variable number tandem repeats, VNTRs) or high-transcribing (five or six VNTRs) polymorphisms, resulting in “high” and “low” genotypes, respectively (Newman et al., 2005). Genotyping of VNTR polymorphisms in *MAOA* was conducted by the Veterinary Genetics Laboratory at UC Davis using polymerase chain reaction (PCR) (Capitanio et al., 2012; Golub et al., 2015; Kinnally et al., 2008). The *MAOA* genotype was included as a variable in this study as it interacts with fluoxetine to affect metabolomics during fluoxetine administration (He et al., 2014). *MAOA* interactions have also been seen in some behaviors, although not for impulsivity (He et al., 2014). Of the animals assigned to each group (treatment and control), half were the high *MAOA* genotype and half were the low *MAOA* genotype.

The treatment group received daily oral administration of fluoxetine (2 mg/kg/d) for two years, during which time growth and behavioral function were evaluated for comparison with the control group receiving vehicle dosing. One year after dosing cessation, behavioral testing was performed before necropsy and tissue sampling.

Impulsivity testing was conducted at two, three, and four years of age (i.e., one and two years after treatment initiation and one year after treatment discontinuation). A reward delay test adapted for monkeys from a similar test for children was performed at UC Davis to measure impulsivity (He et al., 2014). Briefly, monkeys were individually relocated to a separate testing room. The impulsivity test was administered using the Wisconsin General Test Apparatus in a session of 40 trials, which were blinded and randomized for each group. In each experiment, an opaque door opened to expose an opaque movable screen and a test board, on which was placed a transparent plastic box (positioned behind the screen) containing some preferred food items (raisins, miniature marshmallows). The screen moved back 2.54 cm every 2 s. After seven intervals, the food box became fully exposed, at which point the monkey could move the box and obtain the food. If the monkey touched the box before it was fully exposed, the experiment stopped immediately. Impulsivity was calculated based on average number of screen intervals to complete the trial (Ave. Screen) and average latency time and number of trials for the monkey to obtain the reward (Ave. Lat and Ave. Trial, respectively) (He et al., 2014). Impulsivity data from the four-year-old monkeys were used here because the test was performed shortly before brain samples were obtained at necropsy for proteomic analysis and represented residual effects on behavior.

Isolation of macaque brain tissue sections

One month after impulsivity testing of the four-year-old monkeys, brain tissue was collected at necropsy (*N*=12/group). Results of the in life experimental measures have been summarized previously (Golub et al., 2018). Briefly, juvenile monkeys were anesthetized with ketamine (10 mg/kg intramuscularly (i.m.)) and excess pentobarbital (120 mg/kg intravenously (i.v.)), followed by perfusion with 1 L of warm heparinized saline, then 3 L of cold heparinized saline, and a final flush with 500 mL of cold saline. Subsequently, brains were quickly removed and stored in saline for 10 min on ice.

The brains were first cut into 5 mm slices and further into right and left halves along the midsagittal line, with foil placed between the slabs to keep them separated but oriented correctly. For tissue punching, frozen slices were placed on a glass plate chilled with dry ice and DLPFC and CC punches were taken according to the stereotaxic atlas of the rhesus monkey brain (Paxinos et al., 2000). Samples (6–8 punches) were collected using a 1 mm diameter punching needle (Leica Biosystems #39443001RM, Germany). Punches were taken from the cortex of area 6/32 forming the dorsal bank of the cingulate sulcus from slices extending over the frontal planes, bregma +8.00 mm to bregma -7.50 mm. All punches were immediately transferred to a cryovial, frozen in liquid nitrogen, and stored at −80 °C.

Protein sample preparation

The DLPFC (*N*=12/*MAOA* group) and CC tissue punches (*N*=12/*MAOA* group) were lysed in 25 mmol 4-(2-hydroxyethyl)-1-piperazineethanesulfonic acid (HEPES) and 150 mmol NaCl lysis buffer (pH 8.5) with 4% sodium deoxycholate (SDC). The homogenized tissue suspensions were heat-treated for 5 min at 95 °C followed by centrifugation at 18 000 ×*g* for 20 min at 4 °C. For protein concentration determination, supernatants were analyzed using the BCA assay (Thermo Fisher Scientific, USA). The protein extracts were then reduced and alkylated with 100 mmol Tris(2-carboxyethyl)phosphine (TCEP) (Thermo Fisher Scientific, USA) and 400 mmol 2-chloroacetamide (CAM) (Sigma, USA) for 15 min at 45 °C. Reduced and alkylated extracts were treated with Lys-C (Promega, USA) and Trypsin (Serva, Germany) at a ratio of 1:100 (w/w) and digested at 37 °C overnight.

Sample preparation for mass spectrometry

For proteomic analysis, 50 µg of digest was acidified with formic acid (FA) to a final concentration of 5% to remove SDC, then adjusted to pH 7.5–8.0 with 5 mol/L KOH.

For phosphoproteomic analysis, 1 mg of digest was subjected to phosphopeptide enrichment based on the Easy-Phos protocol (Humphrey et al., 2018) with modified steps. Briefly, 400 µL of isopropanol and 100 µL of 48% trifluoroacetic acid (TFA)/8 mmol/L KH_2PO_4 were added to the extracts, followed by complete mixing. Subsequently, 12 mg of TiO_2 beads (GL Sciences, Japan) resuspended in 12 µL of 6% TFA/80% acetonitrile were incubated with the extracts at 40 °C for 5 min. The mixture was centrifuged at 2 000 ×*g* for 1 min at room temperature and the supernatant was discarded. Beads were washed with 1 mL of 5% TFA/60% isopropanol five times to eliminate non-specific binding. After removal of the wash buffer, beads were resuspended in 75 µL of 0.1% TFA/60% isopropanol and loaded onto in-house packed C8 tips (200 µL volume). The samples were centrifuged to dryness at 3 000 ×*g* for 10 min at room temperature. The phosphopeptides on the beads in the C8 tips were eluted (50 µL volume) with 200 µL of ammonia in 800 µL of 40% acetonitrile by centrifugation at 3 000 ×*g* for 10 min at room temperature. Elution was repeated and the eluates were combined and dried in a vacuum centrifuge. Dried samples were reconstituted in 30 µL of HEPES buffer.

Peptides and enriched phosphopeptides were labeled with tandem mass tag (TMT) 10-plex reagent (Thermo Fisher Scientific, USA) according to the manufacturer's protocols. Samples were categorized into four groups based on the *MAOA* genotype and drug treatment of rhesus monkeys (high/flx, high/ctrl, low/flx, and low/ctrl). Each TMT set comprised eight samples (*N*=2/group) and two internal standards, consisting of a pool of all samples. Labeled peptides or phosphopeptides were equally pooled and subjected to prefractionation using a high pH reversed-phase fractionation kit (Thermo Fisher Scientific, USA), resulting in eight proteome peptide fractions and 10 phosphoproteome peptide fractions for each pool. All fractions were collected and evaporated in a vacuum centrifuge and stored at −80 °C until liquid chromatography-tandem mass spectrometry (LC-MS/MS) analysis.

LC-MS/MS analysis

Analysis of fractionated TMT-labeled peptides and phosphopeptides was performed on an Ultimate 3000 UHPLC system (Thermo Fisher Scientific, USA) coupled with a Q-Exactive-Plus mass spectrometer controlled by Xcalibur v4.2.47 (Thermo Fisher Scientific, USA). Briefly, 1 µg of 0.1% FA-resuspended peptides from each fraction was automatically loaded onto a C18 pre-column (300 µm inner diameter (i.d.), Thermo Fisher Scientific, USA) at a flow rate of 10 µL/min (2% acetonitrile/0.1% FA). The 15 cm capillary analytical column (75 µm i.d., New Objective, USA) was packed in-house with 1.9 µm of C18 ReproSil particles (Dr. Maisch GmbH, Germany). The mobile phases used to elute the peptides at 300 nL/min were 0.1% FA as phase A and 95% acetonitrile/0.1% FA as phase B. The 160 min gradient was as follows: pre-equilibration phase with 95% A for 5 min; 5%–30% B for 110 min; 30%–60% B for 20 min; 98% B for 5 min; and post-equilibration with 96% A for 20 min. The LC-MS/MS system was operated in data-dependent acquisition (DDA) mode. Full mass scans were acquired using an Orbitrap mass analyzer in profile mode at a resolution of 70 000 over a range of 375 to 1 400 m/z. The top 10 precursor ions were selected for high energy collision dissociation (HCD) fragmentation with a normalized collision energy (NCE) of 32% and dynamic exclusion time of 30 s. The MS/MS scans were also acquired using the Orbitrap in centroid mode with a resolution of 35 000. The automatic gain control (AGC) targets for full scan and MS/MS were set to 3×10^6 and 1×10^5, respectively. The spray voltage of the electrospray ionization (ESI) source was 1.85 kV and the temperature of the ion transfer capillary was 250 °C.

Raw data processing and bioinformatics analysis

Protein database searches of all raw LC-MS/MS data were performed with Thermo Proteome Discoverer v2.4 (Thermo Fisher Scientific, USA) using the SequestHT search engine against the complete *M. mulatta* (rhesus macaque) sequence database, including all UniProt entries (download 20201103). Spectral selection and most other parameters were set to default. Trypsin was specified as the protease. Mass tolerances for the precursor and fragment ions were set to 10 ppm and 0.02 Da, respectively. Fixed modifications were set

to TMT6 at the N-terminal and lysine (K) residues and carbamidomethyl at the cysteine (C) residues. Methionine (M) oxidation was set as a variable modification for proteomic and phosphoproteomic data analysis. Variable modifications of phosphorylation on serine (S), threonine (T), and tyrosine (Y) were only enabled for phosphoproteomic analysis. Posterior error probabilities (PEPs) were calculated, and peptide spectrum matches (PSMs) were filtered using Percolator v3.0. The false discovery rate (FDR) was estimated using *Q*-value and controlled under 0.05. The IMP-ptmRS algorithm was introduced to localize phosphorylation site sensitivities for phosphoproteomic analysis. For reporter ion quantification in a consensus workflow, raw intensities of unique and razor peptides were extracted, and missing values were imputed using Perseus v1.6.14.10 (Max Planck Institute of Biochemistry, Germany). Data batch effects were corrected using TAMPOR (Johnson et al., 2020) in R (64-bit v4.0.4, https://www.r-project.org/).

Phosphoproteomics dissection using networks (PHOTON) was performed with Perseus v1.6.0.2078 (Max Planck Institute of Biochemistry, Germany) on $\log_2$-transformed normalized phosphopeptide quantities. Differential expression analysis was performed based on two-way analysis of variance (ANOVA) with drug treatment as the first factor and *MAOA* genotype as the second factor, including interactions. Significance was determined based on *P*-values corrected for multiple hypothetical comparisons using the Benjamini-Hochberg method (adjusted *P*-value) with a cutoff value of 0.05. Significant comparison pairs were determined based on *P*-values following Tukey's test for *post-hoc* analysis. Hierarchical cluster analysis was performed for significantly changed proteins and phosphopeptides and a heatmap was created using the R package pheatmap. Correlations between behavioral and proteomics data were performed using the R package Hmisc. Spearman correlation coefficients and significant *P*-values were calculated with linear models. A cutoff of r>0.1 (subtle) or >0.6 (strong) was applied to filter proteins associated with impulsivity.

Gene Ontology (GO) and pathway enrichment analyses were conducted to assign functional annotation to selected (sub)sets or pairs of correlating human homologous genes using the R package clusterProfiler or ClueGO plugin of Cytoscape v3.8.2 (http://www.ici.upmc.fr/cluego/cluegoDownload.shtml). GO enrichment was performed for Cellular Component (CC), Molecular Function (MF), and Biological Process (BP). The annotated pathway database used for analysis was a combination of the Kyoto Encyclopedia of Genes and Genomes (KEGG), Reactome, and WikiPathways databases. The Benjamini-Hochberg-adjusted *P*-value cut-off as set to 0.05. Visualization of GO and pathway enrichment analysis was performed using the R package ggplot2 or network construction in Cytoscape v3.8.2 (https://cytoscape.org/). Functional protein-protein interaction networks were established using STRING v11.0 or imported from the KEGG database using the KEGGparser plugin in Cytoscape v3.8.2 (https://apps.cytoscape.org/apps/cykeggparser). The MCODE (https://apps.cytoscape.org/apps/mcode) and CentiScape plugins (https://apps.cytoscape.org/apps/centiscape) were used to generate subnetworks with Maximal Clique Centrality (MCC) and Degree calculations. The yFiles Layout Algorithms were used to modify the network layout (https://www.yworks.com/products/yfiles-layout-algorithms-for-cytoscape).

RESULTS

Proteomic and phosphoproteomic profiling of DLPFC and CC in rhesus monkeys in response to chronic fluoxetine treatment

The workflow of animals, fluoxetine administration, and behavioral testing prior to LC-MS/MS analysis is shown in Figure 1A. To analyze changes in protein expression and phosphorylation in rhesus monkeys after one year of discontinuation of chronic fluoxetine treatment, we performed quantitative and comprehensive proteomic and phosphoproteomic surveys of the DLPFC and CC (Figure 1B). In total, 5 040 and 5 090 proteins were quantified in the DLPFC and CC, respectively. Of these, 3 656 and 3 413 proteins in corresponding tissue were consistently quantified in all three TMT datasets. For phosphoproteomic analysis, 8 601 and 8 254 phosphopeptides were quantified in the DLPFC and CC, respectively. Of these, 3 674 and 3 894 phosphopeptides were quantified in all three TMT datasets (Figure 1C, <1% FDR). For phosphosite mapping, 8 452 high-confidence phosphosites (Class I site, site probability >75%) from a total of 10 229 phosphosites were quantified in the DLPFC and 8 099 high-confidence phosphosites (Class I site, site probability >75%) out of 9 819 phosphosites were quantified in the CC (Figure 1D). To the best of our knowledge, these data yielded the most comprehensive rhesus monkey proteomic and phosphoproteomic datasets available to date (see Supplementary Data S1).

Protein and phosphopeptide signatures associated with impulsivity

Monkeys chronically treated with fluoxetine for two years (until three years of age) were subjected to impulsivity tests at different ages. We investigated correlations between the proteomic or phosphoproteomic profiles and animal behavior based on linear regression to identify potential biomarkers associated with the impulsivity test data acquired after drug treatment was discontinued but shortly before tissue samples were obtained at four years of age. In the reward delay behavioral test, average number of screen intervals to complete the trial (Ave. Screen) and average latency time and number of trials for the monkeys to obtain the reward (Ave. Lat and Ave. Trial, respectively) were correlated with -omics data ($|r|$>0.6). We identified 21 and 23 proteins associated with impulsivity in the DLPFC and CC, respectively. Protein phosphorylation is an important cellular regulatory mechanism and potential biomarker. In the DLPFC, 25 phosphosites were correlated with impulsivity and phosphorylation of three proteins showed significant correlation. In the CC, 22 phosphosites were linked with impulsivity (Figure 2; Supplementary Data S2).

Differences in proteomes and phosphoproteomes induced by chronic fluoxetine treatment

To identify changes in the DLPFC and CC proteomes and

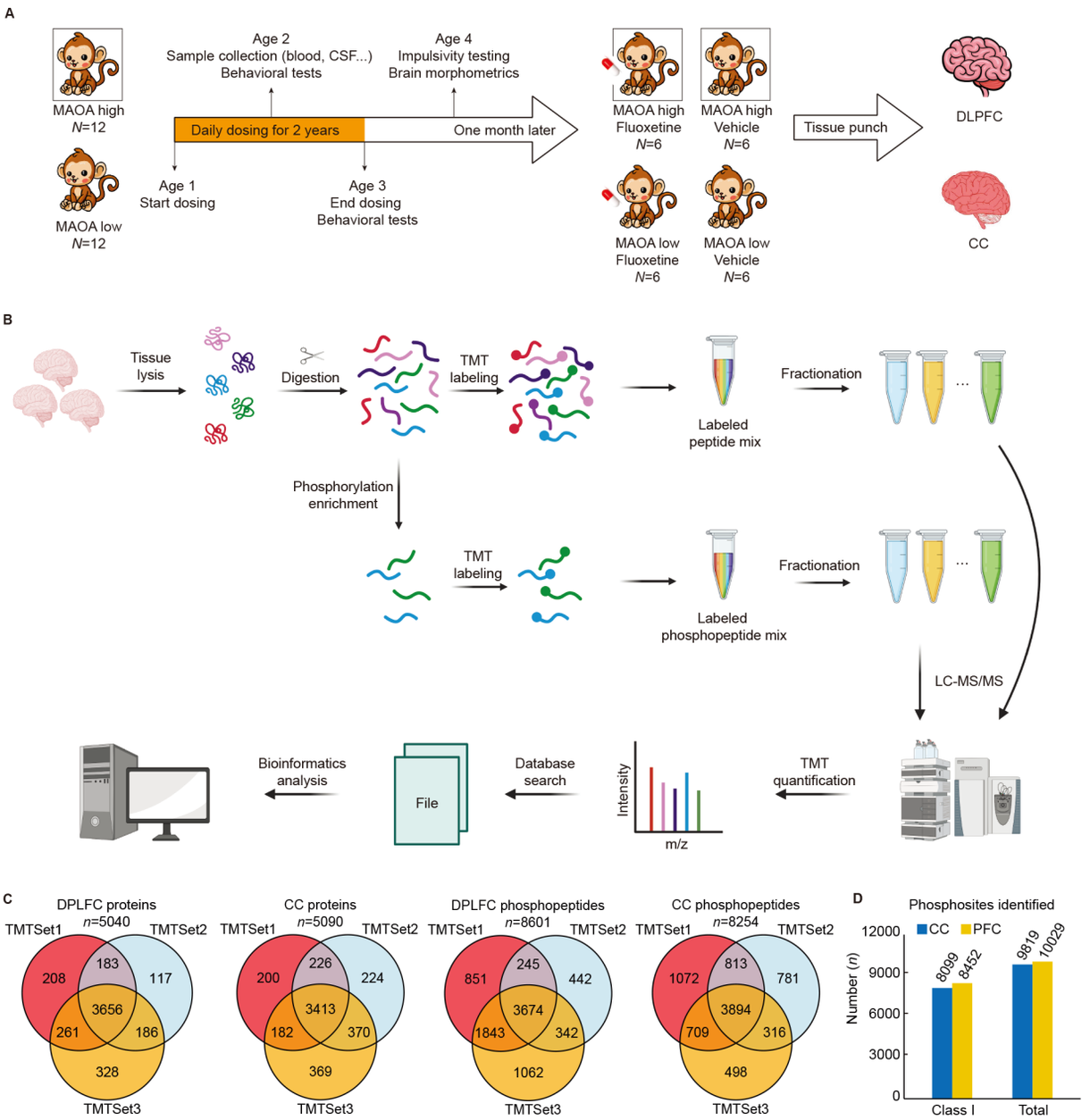

Figure 1 Proteomic and phosphoproteomic study of long-term effects of fluoxetine treatment on juvenile male rhesus monkeys

A: Study protocol and experimental procedures. B: Overview of proteomic and phosphoproteomic profiling. TMT-labeled peptides (proteomic data) and enriched phosphorylated peptides (phosphoproteomic data) were analyzed by LC-MS/MS. C: Proteins and phosphopeptides identified in macaque DLPFC and CC. D: Phosphopeptides identified with >75% site probability (class I site).

phosphoproteomes after chronic fluoxetine treatment in rhesus monkeys, we identified differentially expressed proteins (DEPs) and differentially expressed phosphopeptides (DEpPs) using two-way ANOVA followed by Tukey's test for *post-hoc* analysis, with consideration of the potential interactions between fluoxetine treatment and *MAOA* genotype. In the DLPFC, 79 significant comparison pairs from 39 DEPs were identified using two-way ANOVA (protein fold-change>1.5 and adjusted *P*-value<0.05, Figure 3A). Following fluoxetine treatment, the expression levels of the 39 DEPs showed differences between the high and low *MAOA* genotype monkeys, which were not observed in the vehicle treatment group (Figure 3B). These results suggest that the 39 DEPs identified in the DLPFC could be used to stratify drug responders and non-responders for the two *MAOA* genotypes (see Supplementary Data S3). We also identified 10 DEpPs in the DLPFC, no DEPs in the CC, and 172 DEpPs in the CC, but no biosignatures correlating *MAOA* genotype with drug treatment (Figure 3C).

As most quantified proteins did not show an interaction effect between drug treatment and *MAOA* genotype, we subsequently performed one-way ANOVA followed by Tukey's

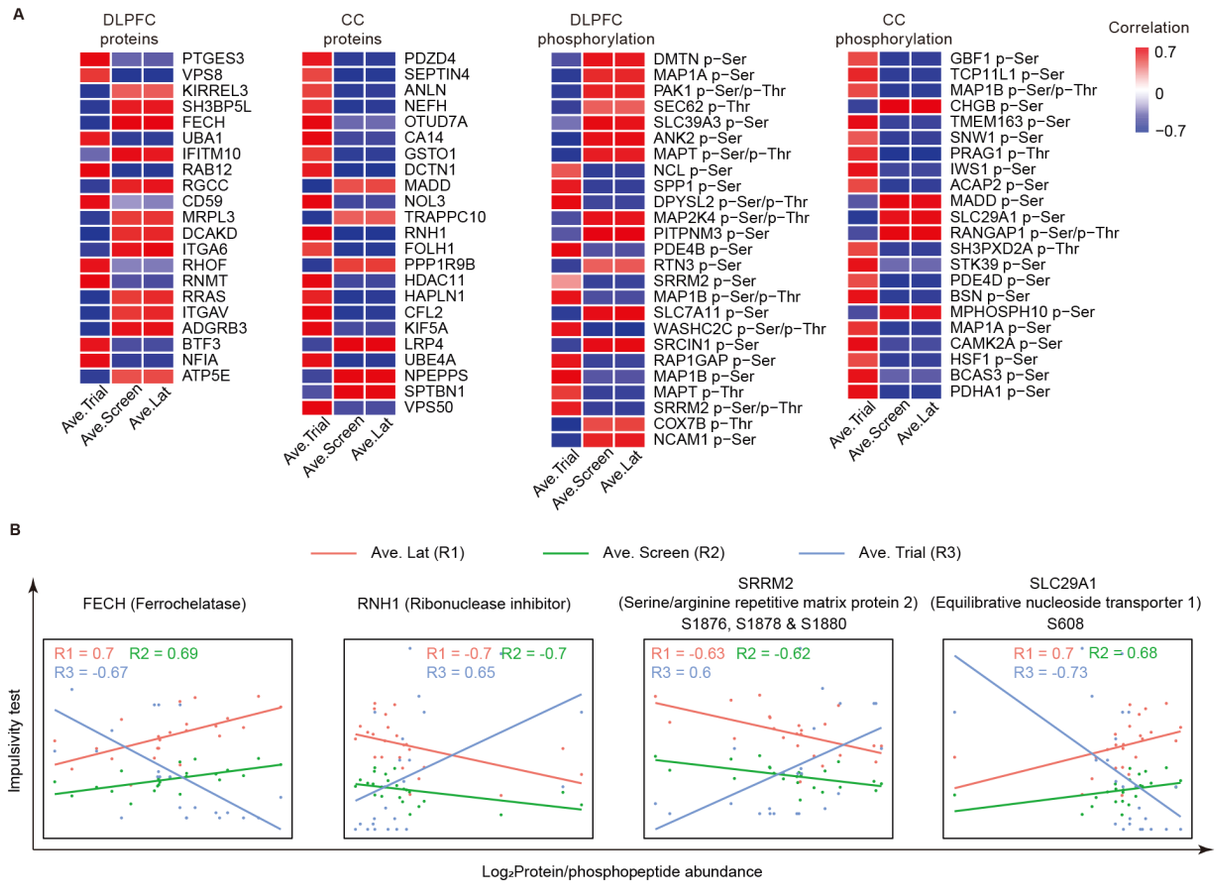

Figure 2 Biomarker candidates associated with impulsivity

Spearman correlation coefficients were calculated. Blue nodes refer to negative correlation and red nodes refer to positive correlation. Color density represents absolute value of correlation coefficients. A: All identified protein and phosphosite biomarkers. B: Correlation between representative proteins and phosphopeptide expression and impulsivity.

test for *post-hoc* analysis to identify proteins and phosphorites that differed between the fluoxetine-treated and control groups without consideration of *MAOA*-genotype interactions, and identified a number of DEPs and DEpPs in the DLPFC and CC (protein fold-change>1.5/phosphopeptide fold-change> 1.3, and adjusted *P*-value<0.05, Figure 3C). Combining significant DEPs/DEpPs with and without *MAOA*-genotype interactions resulted in 471 DEPs and 44 DEpPs in the DLPFC and 134 DEPs and 178 DEpPs in the CC (see Supplementary Data S3). These results indicate that fluoxetine induces significant alterations in the proteomes of both the DLPFC and CC in juvenile rhesus monkeys one year after discontinuation of chronic fluoxetine administration.

Integrated proteomic and phosphoproteomic profiling reveals effects on the GABAergic pathway

We next integrated proteomic and phosphoproteomic data to gain insights into molecular pathways affected by fluoxetine treatment. We first used PHOTON to convert site-specific information into protein-level information (Rudolph et al., 2016). Compared with changes in phosphorylation at specific sites, the derived functional proteins (FPs) allowed for a delineation of affected molecular pathways through integration of proteomic (DEPs) and phosphoproteomic (DEpPs) analysis. Using the PHOTON algorithm, we identified 322 FPs in the DLPFC and 596 FPs in the CC, consistent with our earlier observation that the CC phosphoproteome is more affected than the DLPFC phosphoproteome (see Supplementary Data S3).

We next explored the biological functions affected by fluoxetine and the potential mechanisms underlying increased impulsivity in juvenile rhesus monkeys. We selected DEPs and proteins containing DEpPs and FPs that showed at least a subtle correlation ($|r|$>0.1) with impulsivity. This resulted in four separate protein lists representing differences in the DLPFC and CC proteomes and phosphoproteomes associated with both impulsivity and fluoxetine treatment. Subsequently, GO annotation and pathway analyses were performed on the filtered proteins. In GO enrichment analysis of cellular components, terms enriched in the PHOTON FPs showed higher overall significance than those enriched in DEPs. The most significantly enriched cellular component terms in the CC phosphoproteome were "endoplasmic reticulum lumen" and "glutamatergic synapses". "G-protein beta/gamma-subunit complex" was the most significant term in the DLPFC phosphoproteome, and one of the top enriched terms in both the CC and DLPFC proteomes. Most GO terms enriched in the proteomic proteins were found in multiple

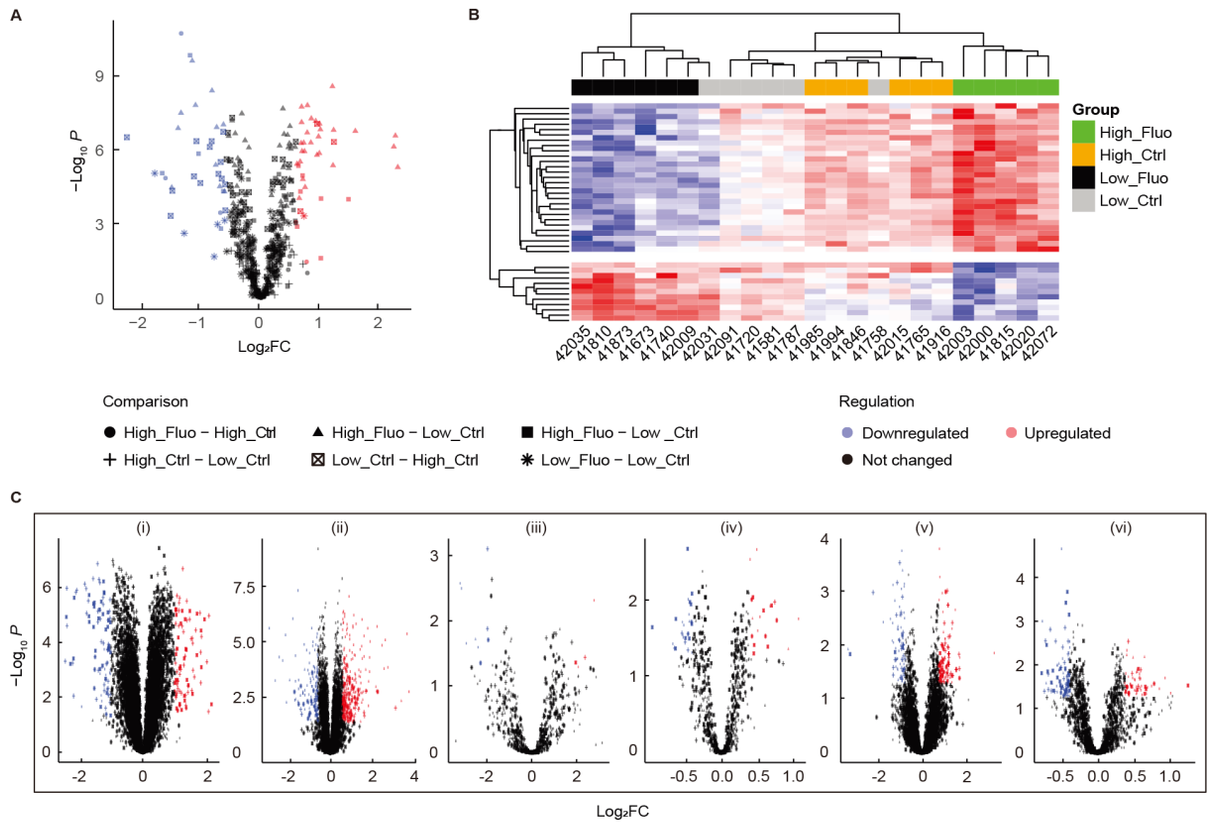

Figure 3 Differential expression analysis of DLPFC and CC proteomes/phosphoproteomes

A: DEPs in DLPFC. B: Heatmap representing expression of 39 regulated proteins identified with *MAOA* genotype-fluoxetine treatment interaction. C: DEPs and DEpPs; DEPs: i) one-way ANOVA (DLPFC), ii) one-way ANOVA (CC), DEpPs: iii) two-way ANOVA (DLPFC), iv) one-way ANOVA (DLPFC), v) two-way ANOVA (CC), and vi) one-way ANOVA (CC).

datasets. "Cytoplasmic side of membrane" and "inner mitochondrial membrane protein complex" were significantly enriched in both the CC and DLPFC (Figure 4A). A similar distribution of GO terms was observed for analysis of molecular function, with the CC phosphoproteome enriched in "voltage-gated calcium channel activity", "G-protein beta-subunit binding", and "regulation of transmembrane transporter activity". The DLPFC phosphoproteome was enriched in many terms related to enzymatic activity, including "regulation of phosphatase activity" and "sodium: potassium-exchanging ATPase activity". Specific terms related to receptor activity enriched in the proteome and phosphoproteome included "NMDA glutamate receptor activity" and "regulation of neurotransmitter receptor activity" (Figure 4A). GO analysis also provided insight into general biological processes affected by fluoxetine. "Post-translational protein modification" was the most enriched process in the CC phosphoproteome, followed by "voltage-gated cation channel activity" and "modulation of chemical synaptic transmission". "Cyclooxygenase pathway" was the most enriched process in response to fluoxetine in the DLPFC phosphoproteome. For the proteomic data, most enriched terms were found in both the CC and DLPFC, including "electron transport chain" and "negative regulation of chromatin silencing" (see Supplementary Figure S1).

To investigate specific pathways associated with fluoxetine-induced increased impulsivity, pathway enrichment was performed against the KEGG, Reactome and WikiPathways databases. "GABAergic synapse" and "Parkinson's disease" showed the highest correlation with increased fluoxetine-related impulsivity in the DLPFC proteome. "Nucleotide excision repair" and "fatty acid metabolism" were the most significantly affected pathways in the DLPFC phosphoproteome and "GABAergic synapse" was also linked to fluoxetine treatment. "GABAergic synapse" was the most relevant pathway in the CC proteome in response to fluoxetine treatment, followed by "signaling by *ERBB2*". "*Ras* signaling pathway" and "GABAergic synapse" were also significantly enriched in the CC phosphoproteome (Figure 4B). To better interpret pathway enrichment analyses, redundant pathways were removed, and the 20 most relevant pathways were selected for further investigation. The heatmaps revealed that the enriched pathways in the phosphoproteomic data were generally more significant than those in the proteomic data, consistent with the GO annotation results (Figure 4C). Several pathways were enriched in multiple datasets, although with varying significance. "GABAergic synapse" was the only pathway enriched in all four datasets, suggesting that the GABAergic synapse-related signaling pathway plays an important role in increased impulsivity after chronic fluoxetine treatment in monkeys.

To study the potential mechanistic mode of action of

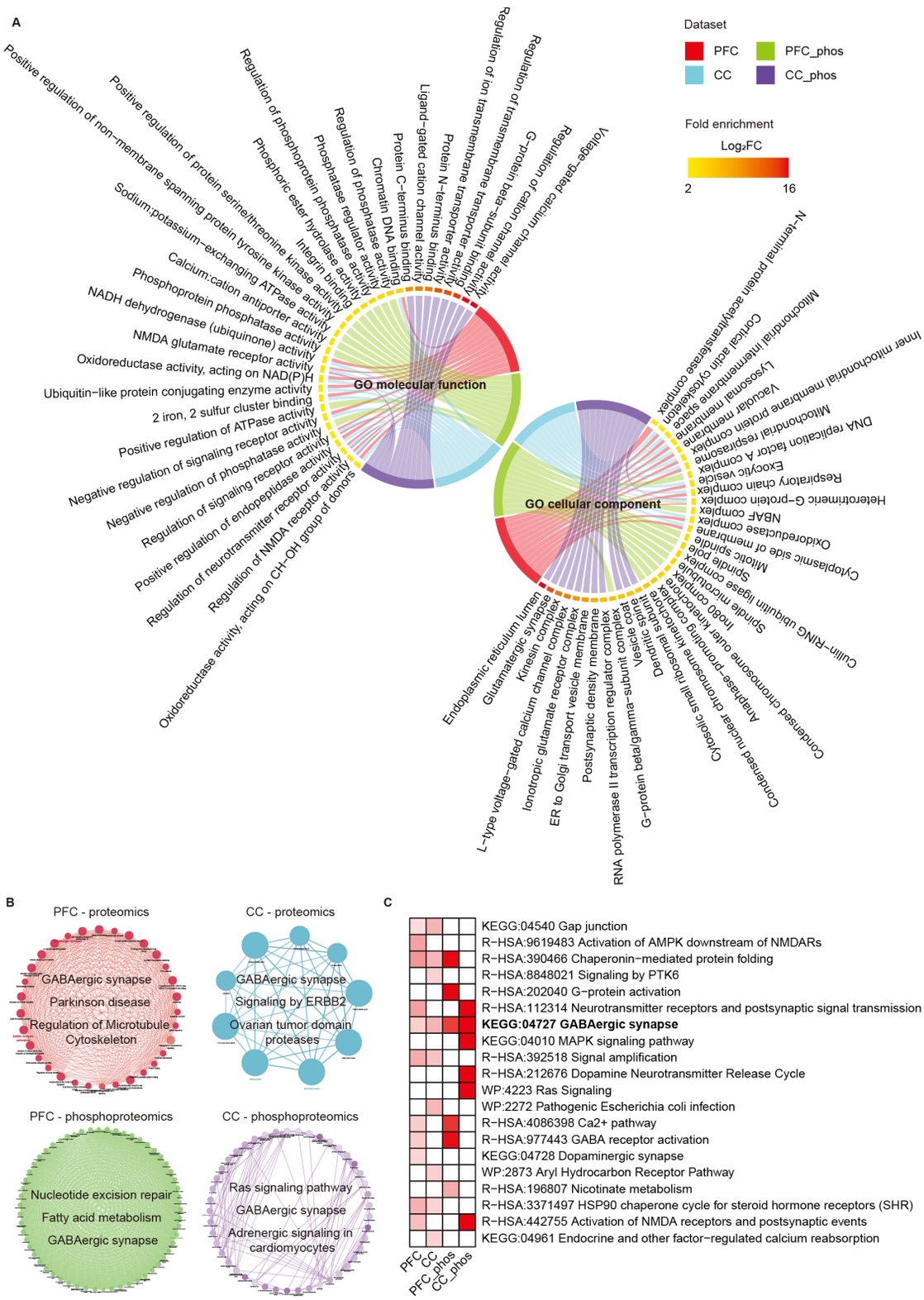

Figure 4 Functional annotation and pathway analyses of DEPs, proteins containing DEpPs, and FPs associated with impulsivity

A: Gene Ontology (GO) annotation in both brain sections for molecular function and cellular component. GO terms were sorted according to adjusted *P*-values. Datasets are represented by different node colors, as indicated in figure. B: Pathway enrichment analysis against KEGG, Reactome, and WikiPathways database. C: Summary of significantly regulated pathways in different datasets. Color density represents adjusted *P*-values from enrichment analysis.

fluoxetine on the GABAergic synapse signaling pathway, all DEPs and parent proteins of DEpPs and FPs identified from the same brain region were integrated and used to construct a protein-protein interaction network underlying the measured responses. In the DLFPC, a total of 60 proteins in the GABAergic signaling pathway associated with increased impulsivity under fluoxetine treatment were included in the protein-protein interaction network annotated using the STRING database (Figure 5A). To identify clusters of highly interconnected proteins, MCODE analysis was applied to the original complex network, yielding one subnetwork cluster consisting of distinct G proteins, GABA B receptors (*GABBR1* and *GABBR2*), metabotropic glutamate receptor 2 (*GRM2*), G protein modulators (*GNGT2* and *GPSM1*), and protein kinase C (*PRKCA PRKCB*, and *PRKCG*). Several topological algorithms, including MCC and Degree, were applied to investigate the subnetwork core. Both MCC and Degree identified 10 G proteins as the most dominant proteins in the whole network. The initial CC network, which included 143 proteins related to impulsivity and fluoxetine treatment, was further clustered into two subnetworks by MCODE analysis (Figure 5A). Consistent with the DLPFC cluster, cluster I in the CC also involved many G proteins and their receptors and modulators both upstream and downstream. Interestingly, cluster II consisted of GABA receptor-binding-related proteins, including three potential biomarkers identified in previous analyses, namely, Ras-related protein Rab-1A (*RAB1A*), spectrin alpha chain (*SPTAN1*), and ankyrin-2 (*ANK2*), indicating that impact on the GABAergic synapse signaling pathway is one of the most significant signatures of fluoxetine treatment. To further simplify the complex cluster I, topological algorithms were used for analysis. Although both MCC and Degree yielded a group of G proteins, the Degree-based network showed the involvement of several downstream kinases, including protein kinase A (*PRKACA* and *PRKACG*), protein kinase C (*PRKCA* and *PRKCB*), and RAC-alpha serine/threonine-protein kinase AKT1.

Our findings showed that G proteins and their receptors and modulators in the DLPFC and CC were affected by fluoxetine treatment, indicating that G-protein signaling, as part of the GABAergic synapse pathway, plays an important role in the mechanism underlying fluoxetine-induced impulsivity in juvenile rhesus monkeys. Subsequently, we analyzed a reconstructed network consisting of G-protein signaling and its main downstream effector, i.e., cyclic adenosine monophosphate (cAMP) signaling pathway. As a result, 95 proteins were involved in the reconstructed network, 44 of which were identified and quantified in our datasets (non-gray nodes). Although most identified proteins in the network were not regulated (green nodes), several key regulators in the two signaling pathways were significantly affected at the proteome or phosphoproteome level, including GABA receptors (*GABRA1*, *GABBR1*, and *GABBR3*), G protein family (Ga, Gi, Go, and Gs), adenylate cyclase (*ADCY1*), protein kinase A (*PRKACA*), and Bcl2-associated agonist of cell death (*BAD*), suggesting that the fluoxetine-induced increase in impulsivity may be associated with the G protein-coupled cAMP signaling pathways. As part of the cAMP signaling pathway, G protein-coupled activation of cAMP and PKA is thought to be activated in developing brains and necessary for the possible contribution of GABA B receptors to neuronal development (Bony et al., 2013; Fiorentino et al., 2009; Gaiarsa & Porcher, 2013; Leung & Wong, 2017). We also found that this pathway was less active in our dataset, as reflected by the down-regulation of key protein expression and phosphorylation levels (PHOTON functional score). Under fluoxetine treatment, the down-regulation of GABA B receptors contributed to the overexpression of Gαi (*GNAI1*, *GNAI2*, and *GNAI3*), i-form α subunits of G proteins known to inhibit adenylyl cyclase (*ADCY1*) activity, resulting in further inhibition of ADCY1 and subsequent decrease in PKA activity. Inhibition of PKA suppresses the activity of Bcl2-associated cell-death agonists, leading to possible cell death. These results indicate that the cAMP-PKA signaling pathway may be an effector of the fluoxetine-induced increase in impulsivity in rhesus monkeys (Figure 5B).

DISCUSSION

Fluoxetine (Prozac™) is the only FDA-approved antidepressant for the treatment of depression in children (>8–14 years of age). Perinatal exposure to fluoxetine can affect brain development in rodents and recent human studies suggest long-term effects on behavior and the brain after fetal exposure during pregnancy (Hutchison et al., 2021). Nonetheless, no studies have been conducted in humans or rodents on the consequences of exposure during childhood (after infancy and before puberty), sometimes termed the “forgotten years”, when important stages of brain development occur (Mah & Ford-Jones, 2012).

Juvenile NHPs are considered appropriate models for human childhood as their brain structure and cognitive and social behaviors undergo extensive maturation during this period. In a previous series of studies, exposure to fluoxetine was shown to influence social, emotional, and cognitive functioning in juvenile rhesus monkeys during and after treatment (Golub et al., 2018). Here, we used proteomics to analyze the brain protein alterations underlying the long-term behavioral effects of fluoxetine exposure in childhood, for which only limited data are currently available (Wang et al., 2019). Large-scale phosphoproteomic studies have shown that dysregulated phosphorylation is a hallmark of many diseases, including a variety of cancers (Zanivan et al., 2013), Alzheimer’s disease (Eidenmüller et al., 2001), and diabetes (Danielsson et al., 2005). However, few studies on psychiatric disorders have been carried out at the phosphoproteomic scale. In the current study, we used comprehensive mass spectrometry as well as behavioral impulsivity and multi-omics data. We performed system-level analysis of the DLPFC and CC proteomes and phosphoproteomes in juvenile rhesus monkeys one year after the discontinuation of three years of fluoxetine treatment to identify associated biomarkers and molecular mechanisms underlying fluoxetine-associated impulsivity. Our rhesus monkey brain proteomic and phosphoproteomic profiling data provide a valuable resource, with a considerable number of novel proteins and phosphorylation sites not represented in public databases (Consortium, 2021; Hornbeck et al., 2015).

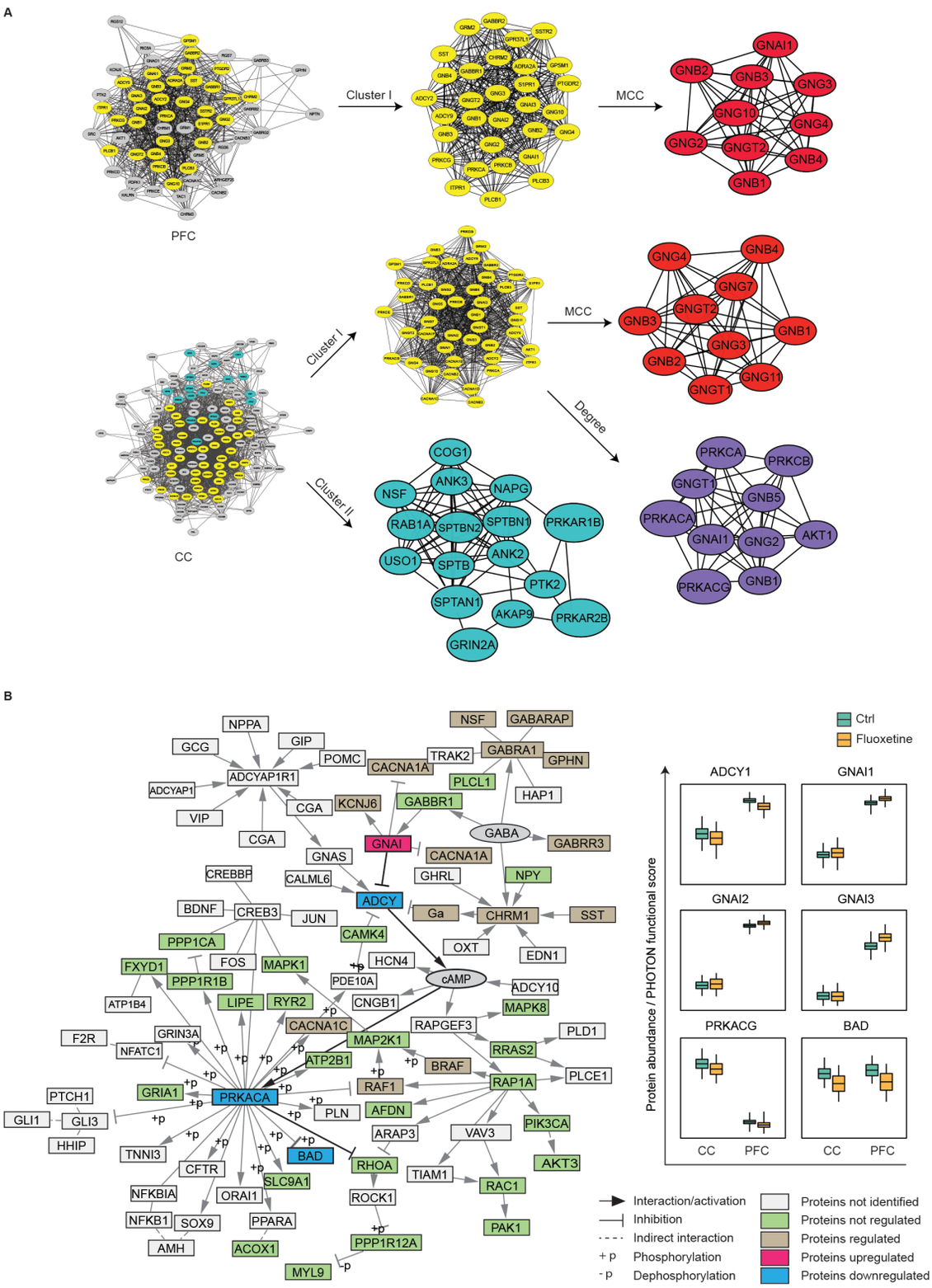

Figure 5 Global network analyses of GABAergic-related DEPs and FPs

A: Reconstructed protein-protein interaction network of DLPFC and CC. Highly interactive subnetwork was extracted using MCODE analysis followed by MCC or Degree analysis. B: cAMP pathways involved in fluoxetine-induced impulsivity increase. Left panel: cAMP signaling pathway; red nodes represent proteins regulated in our data; green nodes represent proteins not regulated in our data; gray nodes represent proteins not identified in our data. Right panel: regulated proteins or phosphoproteins in GABA-cAMP-PKA pathway.

We previously found that fluoxetine treatment can increase impulsivity in juvenile rhesus monkeys based on an assessment of reward delay behavior (He et al., 2014). Combined analysis of impulsivity and proteomic and phosphoproteomic data revealed several protein biomarker candidates associated with fluoxetine treatment and impulsivity, several of which have been reported in previous studies (Dwivedi et al., 2006; Pajer et al., 2012; Shikanai et al., 2018; Yamada & Higuchi, 2002). We also identified several phosphosite biomarkers associated with impulsivity, previously implicated in MDD and impulsivity in other studies (Kékesi et al., 2012; Lopes et al., 2016; Yang et al., 2013, 2014). The biological functions of these biomarker candidates are highly relevant to MDD and brain development and thus deserve further validation.

Although monoamine deficiency is the most prevalent hypothesis for MDD, emerging evidence has implicated GABA deficiency in a hypothetical model of MDD (Mann et al., 2014). Notably, several genes related to the glutamate/GABA system have been reported to be associated with MDD and brain development (Ben-Ari, 2014; Kilb, 2012; Kim & Richardson, 2007; Lazarevic et al., 2019). In our previous metabolomic study, 5-aminovaleric acid lactam, a GABA homolog and weak GABA agonist, was significantly altered in the plasma and CSF of fluoxetine-treated juvenile monkeys, and the metabolism of nicotinamide, which influences GABA receptor activation via the benzodiazepine receptor, was also affected by fluoxetine treatment (Callery & Geelhaar, 1985; He et al., 2014; Möhler et al., 1979). In the current study, we examined perturbations in the proteomes and phosphoproteomes of two brain sections from juvenile monkeys after long-term fluoxetine treatment. Consistent with our previous metabolomic profiling study, proteins and phosphorylation events related to GABAergic synapses were involved in the response of juvenile monkeys to fluoxetine treatment. Notably, fluoxetine treatment induced the down-regulation of the GABA B receptor, a key regulator of membrane excitability and synaptic transmission in the brain, in both the DLPFC and CC. The GABA B receptor is a G protein-coupled receptor associated with a subset of G proteins (pertussis toxin sensitive Gi/o family) that regulate specific ion channels and trigger cAMP cascades. Overexpression of Gαi proteins (*GNAI1*, *GNAI2*, and *GNAI3*) was also observed following the down-regulation of the GABA B receptor, which further induced the inhibition of ADCY, a family of proteins that can synthesize cAMP from adenosine triphosphate (ATP). Consequently, inhibition of ADCY affected the activation of downstream cAMP-PKA signaling pathway-associated biological processes, probably via gene transcription. However, further investigation is required to validate the proposed model and explore how it alters brain development.

CONCLUSIONS

We established the proteomic and phosphoproteomic profiles of the DLPFC and CC in juvenile rhesus monkeys after long-term fluoxetine treatment and discontinuation of drug administration. We identified several biomarker candidates and the GABAergic synapse pathway as a potential mechanism underlying fluoxetine-induced impulsivity. Our study provides a useful proteomic resource that may benefit research on NHP brain development. Following verification, the identified biomarkers and molecular pathways may also assist in studying the long-term effects of fluoxetine and in the development of novel antidepressants with fewer side effects.

DATA AVAILABILITY

The LC-MS/MS raw data reported in this paper have been deposited in OMIX, China National Center for Bioinformation/Beijing Institute of Genomics, Chinese Academy of Sciences (https://ngdc.cncb.ac.cn/omix, accession no. OMIX001759), Science Data Bank (https://www.scidb.cn/en, DOI: 10.57760/sciencedb.j00139.00037), and Mass Spectrometry Interactive Virtual Environment (MassIVE, https://massive.ucsd.edu, MSV000090283) (Chen et al., 2021; CNCB-NGDC Members and Partners, 2022).

SUPPLEMENTARY DATA

Supplementary data to this article can be found online.

COMPETING INTERESTS

The authors declare that they have no competing interests.

AUTHORS' CONTRIBUTIONS

C.W.T. and M.G. conceived and designed the project. Y.Y., A.H., and D.I.P. performed the experiments. Y.Y. and C.W.T. analyzed the data. C.W.T. and M.G. supervised the work. All authors contributed to writing the manuscript. All authors read and approved the final version of the manuscript.

ACKNOWLEDGMENTS

We appreciate the contribution of Casey Hogrefe and the Anatomic and Clinical Pathology group at the California National Primate Research Center for the collection and shipping of brain tissue samples.

REFERENCES

Ballif BA, Villén J, Beausoleil SA, Schwartz D, Gygi SP. 2004. Phosphoproteomic analysis of the developing mouse brain. *Molecular & Cellular Proteomics*, **3**(11): 1093−1101.

Ben-Ari Y. 2014. The GABA excitatory/inhibitory developmental sequence: a personal journey. *Neuroscience*, **279**: 187−219.

Bony G, Szczurkowska J, Tamagno I, Shelly M, Contestabile A, Cancedda L. 2013. Non-hyperpolarizing $GABA_B$ receptor activation regulates neuronal migration and neurite growth and specification by cAMP/LKB1. *Nature Communications*, **4**: 1800.

Bromet E, Andrade LH, Hwang I, Sampson NA, Alonso J, De Girolamo G, et al. 2011. Cross-national epidemiology of DSM-IV major depressive episode. *BMC Medicine*, **9**: 90.

Callery PS, Geelhaar LA. 1985. 1-piperideine as an in vivo precursor of the γ-aminobutyric acid homologue 5-aminopentanoic acid. *Journal of Neurochemistry*, **45**(3): 946−948.

Capitanio JP, Del Rosso LA, Calonder LA, Blozis SA, Penedo MCT. 2012. Behavioral effects of prenatal ketamine exposure in rhesus macaques are

dependent on MAOA genotype. *Experimental and Clinical Psychopharmacology*, **20**(3): 173−180.

Carlyle BC, Kitchen RR, Kanyo JE, Voss EZ, Pletikos M, Sousa AMM, et al. 2017. A multiregional proteomic survey of the postnatal human brain. *Nature Neuroscience*, **20**(12): 1787−1795.

Chen TT, Chen X, Zhang SS, Zhu JW, Tang BX, Wang AK, et al. 2021. The genome sequence archive family: toward explosive data growth and diverse data types. *Genomics, Proteomics & Bioinformatics*, **19**(4): 578−583.

CNCB-NGDC Members and Partners. 2022. Database resources of the national genomics data center, China National Center for bioinformation in 2022. *Nucleic Acids Research*, **50**(D1): D27−D38.

Costello EJ, Mustillo S, Erkanli A, Keeler G, Angold A. 2003. Prevalence and development of psychiatric disorders in childhood and adolescence. *Archives of General Psychiatry*, **60**(8): 837−844.

Danielsson A, Öst A, Nystrom FH, Strålfors P. 2005. Attenuation of insulin-stimulated insulin receptor substrate-1 serine 307 phosphorylation in insulin resistance of type 2 diabetes. *Journal of Biological Chemistry*, **280**(41): 34389−34392.

Doubleday PF, Ballif BA. 2014. Developmentally-dynamic murine brain proteomes and phosphoproteomes revealed by quantitative proteomics. *Proteomes*, **2**(2): 191−207.

Dwivedi Y, Mondal AC, Rizavi HS, Faludi G, Palkovits M, Sarosi A, et al. 2006. Differential and brain region–specific regulation of Rap-1 and Epac in depressed suicide victims. *Archives of General Psychiatry*, **63**(6): 639−648.

Eidenmüller J, Fath T, Maas T, Pool M, Sontag E, Brandt R. 2001. Phosphorylation-mimicking glutamate clusters in the proline-rich region are sufficient to simulate the functional deficiencies of hyperphosphorylated tau protein. *Biochemical Journal*, **357**(3): 759−767.

Fiorentino H, Kuczewski N, Diabira D, Ferrand N, Pangalos MN, Porcher C, et al. 2009. $GABA_B$ receptor activation triggers BDNF release and promotes the maturation of GABAergic synapses. *Journal of Neuroscience*, **29**(37): 11650−11661.

Gaiarsa JL, Porcher C. 2013. Emerging neurotrophic role of $GABA_B$ receptors in neuronal circuit development. *Frontiers in Cellular Neuroscience*, **7**: 206.

Golub MS, Bulleri AM, Hogrefe CE, Sherwood RJ. 2015. Bone growth in juvenile rhesus monkeys is influenced by 5HTTLPR polymorphisms and interactions between 5HTTLPR polymorphisms and fluoxetine. *Bone*, **79**: 162−169.

Golub MS, Hackett EP, Hogrefe CE, Leranth C, Elsworth JD, Roth RH. 2017. Cognitive performance of juvenile monkeys after chronic fluoxetine treatment. *Developmental Cognitive Neuroscience*, **26**: 52−61.

Golub MS, Hogrefe CE. 2016. Sleep disturbance as detected by actigraphy in pre-pubertal juvenile monkeys receiving therapeutic doses of fluoxetine. *Neurotoxicology and Teratology*, **55**: 1−7.

Golub MS, Hogrefe CE, Bulleri AM. 2016a. Peer social interaction is facilitated in juvenile rhesus monkeys treated with fluoxetine. *Neuropharmacology*, **105**: 553−560.

Golub MS, Hogrefe CE, Bulleri AM. 2016b. Regulation of emotional response in juvenile monkeys treated with fluoxetine: MAOA interactions. *European Neuropsychopharmacology*, **26**(12): 1920−1929.

Golub MS, Hogrefe CE, Campos LJ, Fox AS. 2019. Serotonin transporter binding potentials in brain of juvenile monkeys 1 year after discontinuation of a 2-year treatment with fluoxetine. *Biological Psychiatry:Cognitive Neuroscience and Neuroimaging*, **4**(11): 948−955.

Golub MS, Hogrefe CE, Sherwood RJ, Turck CW. 2018. Fluoxetine administration in juvenile monkeys: implications for pharmacotherapy in children. *Frontiers in Pediatrics*, **6**: 21.

He Y, Hogrefe CE, Grapov D, Palazoglu M, Fiehn O, Turck CW, et al. 2014. Identifying individual differences of fluoxetine response in juvenile rhesus monkeys by metabolite profiling. *Translational Psychiatry*, **4**(11): e478.

Hornbeck PV, Zhang B, Murray B, Kornhauser JM, Latham V, Skrzypek E. 2015. PhosphoSitePlus, 2014: mutations, PTMs and recalibrations. *Nucleic Acids Research*, **43**(D1): D512−D520.

Humphrey SJ, Karayel O, James DE, Mann M. 2018. High-throughput and high-sensitivity phosphoproteomics with the EasyPhos platform. *Nature Protocols*, **13**(9): 1897−1916.

Hutchison SM, Mâsse LC, Pawluski JL, Oberlander TF. 2021. Perinatal selective serotonin reuptake inhibitor (SSRI) and other antidepressant exposure effects on anxiety and depressive behaviors in offspring: A review of findings in humans and rodent models. *Reproductive Toxicology*, **99**: 80−95.

Johnson ECB, Dammer EB, Duong DM, Ping LY, Zhou MT, Yin LM, et al. 2020. Large-scale proteomic analysis of Alzheimer's disease brain and cerebrospinal fluid reveals early changes in energy metabolism associated with microglia and astrocyte activation. *Nature Medicine*, **26**(5): 769−780.

Kékesi KA, Juhász G, Simor A, Gulyássy P, Szegő ÉM, Hunyadi-Gulyás É, et al. 2012. Altered functional protein networks in the prefrontal cortex and amygdala of victims of suicide. *PLoS One*, **7**(12): e50532.

Kilb W. 2012. Development of the GABAergic system from birth to adolescence. *The Neuroscientist*, **18**(6): 613−630.

Kim JH, Richardson R. 2007. A developmental dissociation of context and GABA effects on extinguished fear in rats. *Behavioral Neuroscience*, **121**(1): 131−139.

Kinnally EL, Lyons LA, Abel K, Mendoza S, Capitanio JP. 2008. Effects of early experience and genotype on serotonin transporter regulation in infant rhesus macaques. *Genes, Brain and Behavior*, **7**(4): 481−486.

Lazarevic V, Mantas I, Flais I, Svenningsson P. 2019. Fluoxetine suppresses glutamate- and GABA-mediated neurotransmission by altering SNARE complex. *International Journal of Molecular Sciences*, **20**(17): 4247−4247.

Leung CCY, Wong YH. 2017. Role of G protein-coupled receptors in the regulation of structural plasticity and cognitive function. *Molecules*, **22**(7): 1239.

Lopes S, Vaz-Silva J, Pinto V, Dalla C, Kokras N, Bedenk B, et al. 2016. Tau protein is essential for stress-induced brain pathology. *Proceedings of the National Academy of Sciences of the United States of America*, **113**(26): E3755−E3763.

Mah VK, Ford-Jones EL. 2012. Spotlight on middle childhood: rejuvenating the 'forgotten years'. *Paediatrics & Child Health*, **17**(2): 81−83.

Mann JJ, Oquendo MA, Watson KT, Boldrini M, Malone KM, Ellis SP, et al. 2014. Anxiety in major depression and cerebrospinal fluid free gamma-aminobutyric acid. *Depression and Anxiety*, **31**(10): 814−821.

Möhler H, Polc P, Cumin R, Pieri L, Kettler R. 1979. Nicotinamide is a brain constituent with benzodiazepine-like actions. *Nature*, **278**(5704): 563−565.

Newman TK, Syagailo YV, Barr CS, Wendland JR, Champoux M, Graessle M, et al. 2005. Monoamine oxidase A gene promoter variation and rearing experience influences aggressive behavior in rhesus monkeys. *Biological Psychiatry*, **57**(2): 167−172.

Pajer K, Andrus BM, Gardner W, Lourie A, Strange B, Campo J, et al. 2012. Discovery of blood transcriptomic markers for depression in animal models and pilot validation in subjects with early-onset major depression.

Translational Psychiatry, **2**(4): e101.
Paxinos G, Huang XF, Toga AW. 2000. The Rhesus Monkey Brain in Stereotaxic Coordinates. San Diego: Academic Press.
Reite M, Short R. 1983. Maternal separation studies: rationale and methodological considerations. *Progress in Clinical and Biological Research*, **131**: 219−253.
Rudolph JD, De Graauw M, Van De Water B, Geiger T, Sharan R. 2016. Elucidation of signaling pathways from large-scale phosphoproteomic data using protein interaction networks. *Cell Systems*, **3**(6): 585−593.e3.
Schildkraut JJ. 1965. The catecholamine hypothesis of affective disorders: a review of supporting evidence. *American Journal of Psychiatry*, **122**(5): 509−522.
Selph SS, McDonagh MS. 2019. Depression in children and adolescents: evaluation and treatment. *American Family Physician*, **100**(10): 609−617.
Shikanai M, Yuzaki M, Kawauchi T. 2018. Rab family small GTPases-mediated regulation of intracellular logistics in neural development. *Histology and Histopathology*, **33**(8): 765−771.
Su SY, Hogrefe-Phi CE, Asara JM, Turck CW, Golub MS. 2016. Peripheral fibroblast metabolic pathway alterations in juvenile rhesus monkeys undergoing long-term fluoxetine administration. *European Neuropsychopharmacology*, **26**(7): 1110−1118.
The UniProt Consortium. 2021. UniProt: the universal protein knowledgebase in 2021. *Nucleic Acids Research*, **49**(D1): D480−D489.
Tkachev A, Stekolshchikova E, Bobrovskiy DM, Anikanov N, Ogurtsova P, Park DI, et al. 2021. Long-term fluoxetine administration causes substantial lipidome alteration of the juvenile macaque brain. *International Journal of Molecular Sciences*, **22**(15): 8089.
von Knorring AL, Bohman M, von Knorring L, Oreland L. 1985. Platelet MAO activity as a biological marker in subgroups of alcoholism. *Acta Psychiatrica Scandinavica*, **72**(1): 51−58.
Wang H, Diaz AK, Shaw TI, Li YX, Niu MM, Cho JH, et al. 2019. Deep multiomics profiling of brain tumors identifies signaling networks downstream of cancer driver genes. *Nature Communications*, **10**(1): 3718.
Yamada M, Higuchi T. 2002. Functional genomics and depression research: beyond the monoamine hypothesis. *European Neuropsychopharmacology*, **12**(3): 235−244.
Yang C, Guo X, Wang GH, Wang HL, Liu ZC, Liu H, et al. 2014. Changes in tau phosphorylation levels in the hippocampus and frontal cortex following chronic stress. *Brazilian Journal of Medical and Biological Research*, **47**(3): 237−244.
Yang Y, Yang D, Tang G, Zhou C, Cheng K, Zhou J, et al. 2013. Proteomics reveals energy and glutathione metabolic dysregulation in the prefrontal cortex of a rat model of depression. *Neuroscience*, **247**: 191−200.
Zanivan S, Meves A, Behrendt K, Schoof EM, Neilson LJ, Cox J, et al. 2013. In vivo SILAC-based proteomics reveals phosphoproteome changes during mouse skin carcinogenesis. *Cell Reports*, **3**(2): 552−566.